GIANT-IMPACT FORMING THE CRUSTAL THICKNESS DICHOTOMY OF THE MOON. M. -H. Zhu[1], K. Wünnemann[2], [1]Space Science Institute, Macau University of Science and Technology, Taipa, Macau (mhzhu@must.edu.mo), [2]Museum für Naturkunde, Leibniz Institute for Evolution and Biodiversity Science, Berlin, Germany.

Introduction: The dichotomy of crustal thickness is one of the striking feature of the Moon. Recent observations from the GRAIL mission indicate a crustal thickness of ~ 30-40 km on the nearside lowlands and ~ 50-60 km on the farside highlands [1]. The highland crust may be composed of two layers: a primary anorthositic crust with a thickness ~ 30-50 km, and an uppermost mafic-rich layer with a thickness of ~ 10 km [2]. Several mechanisms [3-8] have been proposed to explain the formation of the crustal thickness dichotomy, but the origin remains controversial. Giant impacts are thought to have happened frequently in the ancient solar system and the collision of a large body with Mars has been suggested as an explanation for the north-south crustal dichotomy on Mars [9]. Therefore, it is possible that the ancient Moon suffered from a giant impact, which could have formed the Moon's crustal thickness dichotomy and farside highlands. For this work, we conducted a series of numerical models of giant impacts on the Moon to test quantitatively the large collision hypothesis for the formation of crustal dichotomy and farside highlands.

Methods: We used the iSALE shock-physics code [10] to simulate giant impacts. In our models the Moon is approximated by a 3,500-km-dimater sphere with 700-km-diameter iron core. The crustal thickness is assumed to be 50 km. We use gabbroic anorthosite and dunite to represent the lunar crust and mantle. The former is also used for the projectile. Since giant impacts are strongly affected by the temperature gradient of the target [11], we use two possible thermal profiles that may be realistic for the anciant Moon. Thermal profile 1 (TP1) has a crust and upper mantle temperature gradient of 10 K km^{-1}; the temperature follows the mantle solidus between a depth of 150-350 km, which would cause partial melting of the upper mantle at this depth range; in the deep mantle (> 350 km depth) the temperature reaches 1670 K and remains constant [12]. Thermal profile 2 (TP2) has a crustal gradient of 30 K km^{-1}, representing a 0.5 Giga-year-old Moon, in which the whole interior is not far from the mantle solidus [11]. We do not consider a thermal profile of the impactor and simulate head-on collisions, only. We varied the size of the impactor between 400 km and 1000 km in diameter, and the impact velocity between 3 km s^{-1} and 17 km s^{-1}. Self-gravity was not considered in the simulations, as some preliminary test-runs indicate that the effect may be negligible. In all the models, the impact site was assumed at 15° N, 23° W, corresponding to the center of Procellarum basin [13].

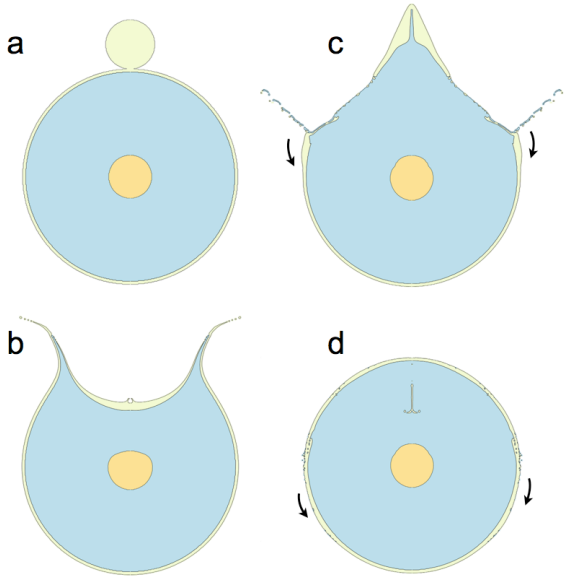

Fig. 1 Snapshots of crater formation for a giant-impact (diameter of 800 km and velocity of ~ 8.0 km s^{-1}) on the Moon. The arrows in (c) and (d) indicate the movement and bulking of crustal material during the impact cratering process.

Results: Fig. 1 illustrates the basin-forming process for an impactor of 800 km in diameter with an impact velocity of ~ 8.0 km s^{-1} for TP2 (Fig. 1a). In the first ten minutes, the impactor penetrates into the target, displaces and excavates target material, and forms a transient crater, ~ 1800 km in radius and ~ 1200 km in depth; the floor of the transient crater is covered with a thick veneer of projectile and crustal material (Fig. 1b). The crater collapse begins with an upwards movement of the crater floor forming a central peak several hundred kilometers high while the diameter of the transient cavity continues to increase. After 45 minutes, the hot central uplift starts to collapse back into the crater. The downwards and outwards material flow pushes crustal material in a radial direction resulting in a thickened crustal region comparable in extent to the farside highlands (Fig. 1c). After approximately 220 minutes central uplift collapse has ceased and the subsequent migration of crustal and mantle material around the basin fills the excavated cavity with the melt pool covering the inner part of the basin (~ 2500 km in radius). The surrounding proximal ejecta slump

back into the basin and do not remain as a thick ejecta blanket and elevated crater rim in the proximity of the crater. Therefore, the specific morphologic features of basin structures are eliminated (Fig. 1d). Impactor material mixed with crustal material remains on top inside the basin, forming a new ~ 30 km thick crust.

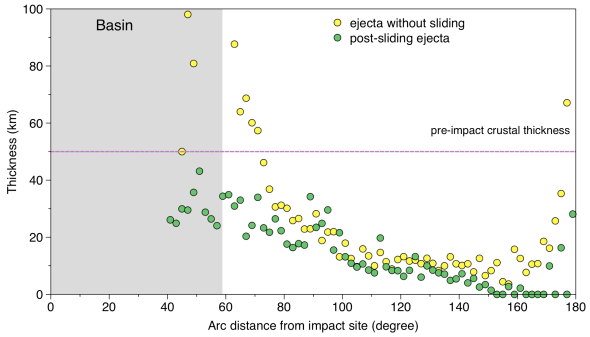

Fig. 2 The sliding effect of the ejecta thickness variation along the arc distance from the impact site. The gray part represents the transient crater size.

The ejecta thickness was calculated by the hyperparabolic trajectory continuation of ejected tracers [14]. The surrounding surface of the basin was subdivided into 2-degree arc discrete rings. The calculated ejecta thickness is ~ 140 km at the transient crater rim, then decreases to 11 km at an arc distance of 100 degree from the basin center (Fig. 2). To further arc distance of 170 degree, the ejecta thickness retains 10-15 km, but increases rapidly to 250 km at the antipode of the impact site. The ejecta, once landed, were assumed to be transported in the same way as other material at its landing site and its movement was tracked to calculate the post-sliding location. The ejected mantle material that moved back into the transient crater was not considered to contribute to the formation of a new crust. The post-sliding ejecta thickness is 10-15 km on the farside, ~ 90 % of which is mantle material. Mantle material dominates the composition of the ejecta blanket, which may explain the observed uppermost mafic-rich mixed layer on the farside highlands [2].

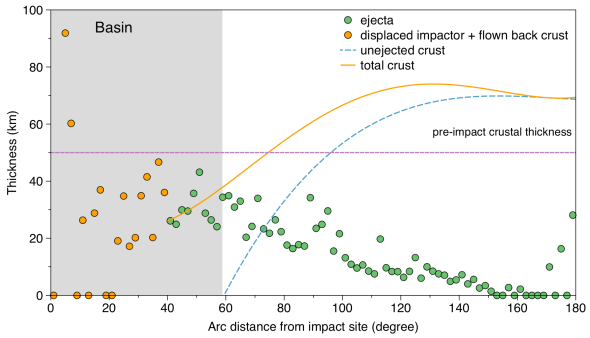

Fig. 3 The modeled crust, including the post-sliding ejecta and unejected crust. The gray part represents the transient crater size.

The modeled crustal thickness was calculated by adding the post-sliding ejecta thickness to the unejected crust. Fig. 3 shows the variation of the modeled crustal thickness along the arc distance from impact site. The modeled crustal thickness increases from ~ 30 km at the basin boundary to ~ 60 km at an arc distance of 90 degree from the basin center, reaching a maximum value of 75 km at an arc distance of 130 degree. The crustal thickness then decreases slowly to ~ 70 km at an arc distance of 170 degree. At the antipode (170 - 180 degree), the post-sliding ejecta has a high variation in thickness from 0 to 30 - 40 km, therefore was not included in the calculation of the new crustal thickness.

Discussion: In the proposed giant impact scenario a crater structure is formed but does not preserve the specific morphological features of other basins that are smaller and were formed subsequently in the evolution of the Moon. The boundary of the modeled transient crater (~ 1800 km in radius) corresponds to the size of the PKT [15] and the rim of the final crater is located at the boundary between farside and nearside. The impact forms the new crust with a thickness of ~ 30 km on the nearside and ~ 60-70 km on the farside, which is roughly consistent with the crustal thickness model derived from the gravity observations [1].

The giant impact event forms a new crust with thickness of 60 - 70 km within the SPA terrain (~170-180 arc distance in Fig. 3). Although the impact event forming the SPA basin excavates voluminous material [14], the giant impact scenario on the nearside forming the crustal dichotomy of the Moon implies that ejecta from the SPA basin had a small effect on the farside highlands. Additionally, the larger crustal thickness within the SPA terrain (60-70 km) might be the reason that the oblique SPA basin-forming impact may not excavate the mantle material [16].

References: [1] Wieczorek M. et al. (2013) *Science*, *339*, 671-675. [2] Yamamoto S. et al. (2012) *GRL*, *39*, L13201. [3] Wood J. A. (1973) *Moon*, *8*, 73-103. [4] Loper D. E. and Werner C. L. (2002) *JGR*, *107*, 5046. [5] Wasson J. T. and Warran P. H. (1980) *Icarus*, *44*, 752-771. [6] Zuber M. et al. (1994) *Science*, *266*, 1839-1843. [7] Garrick-Bethell I. et al. (2010) *Science*, *330*, 949-951. [8] Jutzi M. and Asphaug E. (2011) *Nature*, *476*, 69 – 72. [9] Andrews-Hanna J. C. et al. (2008) *Nature*, *514*, 68 – 71. [10] Amsden A. et al. (1980) *LANL Rep. LA-8095*, Los Alamos Natl. Lab. [11] Ivanov B. et al. (2010) *Large Meteorite Impacts and Planetary Evolution IV*, 29-49. [12] Potter R. W. et al. (2012) *Icarus*, *220*, 730-743. [13] Whitaker E. A. (1981) *LPSC.*, *12A*, 105-111. [14] Zhu M. –H. et al. (2015) *JGR*, 10.1002/2015JE004827. [15] Jolliff B. et al. (2000) *JGR*, *105*, 4197-4216. [16] Melosh J. et al. (2014) *LPSC*, Abstract #2505.